Efficiency and Cost Trade-Offs for Designing Module Integrated Converter Photovoltaic Systems

Katherine A. Kim, Sutchaya Lertburapa, Chenyang Xu, and Philip T. Krein
Department of Electrical and Computer Engineering
University of Illinois at Urbana-Champaign
Urbana, IL, USA

***Abstract*—Photovoltaic (PV) systems are moving away from the traditional series-string PV structure and towards a module-integrated-converter (MIC) configuration for improved energy capture. A MIC approach trades off increased power production with increased cost and overhead power consumption. This research compares efficiency and cost of series-string, micro-converter, and micro-inverter PV system configurations. Analytical models for power production, cost, and cost per watt are developed for each configuration. Design choices such as the current sensor type, microcontroller, and maximum power point tracking (MPPT) algorithm affect power production and cost. Various design cases are explored to identify the number of MICs that minimize system cost per watt.**

I. Introduction

Photovoltaic (PV) systems can be constructed in a variety of configurations to capture solar energy and provide power to the grid. Traditionally, PV panels are strung in series and connected to a central inverter. Within the inverter, there is a dc-dc converter stage to control PV operation and a dc-ac inverter stage to synchronize with the grid, as shown in Fig. 1(a). Cell mismatch due to differences in manufacturing, temperature, shading, and degradation results in uneven power generation. This compromises total power production and can reduce potential gains by 5-10% [1].

To minimize string mismatch losses, the power electronics and control can be integrated into the PV module, called a *module integrated converter* (MIC). This allows for more localized control such that each panel can independently operate at its maximum power point (MPP), providing higher total power [2]. Moving only the dc-dc converter into the PV module creates a *micro-converter* (MC) configuration, as shown in Fig. 1(b). Additionally, moving the inverter into the module makes a *micro-inverter* (MI) configuration, as shown in Fig. 1(c). Series-string configurations are still the most common configuration, but MICs are growing in popularity.

A modular approach allows for improved efficiency, lower initial investment, and scalability. As the power electronics move closer to the cell level, more modules are necessary for the same system power rating. Each converter consists of a power stage, controller, sensors, and signal conditioning circuitry; all of which consume power. Thus, there is a benefit to decreasing component cost and overhead energy consumption in each converter [3]. There is a basic trade-off between the increased power gained from smaller modules and increased cost. For a given dc-dc converter and inverter design, the optimal number converter modules can be found that minimizes system cost per watt. To capture lifetime cost per watt of a PV system, factors such as power degradation and maintenance costs should be considered [4]. However, this study focuses on the equipment costs, which are straightforward to quantify and adequate for basic comparison purposes.

This paper develops analytical models for series-string, MC, and MI system power consumption and cost. The models are used to determine the power production efficiency under nominal conditions and total equipment cost for a 10 kW residential system. Through this analysis, gains achieved by using a MIC approach are demonstrated. Test cases are used to compare a number of design choices and find the lowest cost per watt and associated number of modules.

II. Power Consumption and Cost Model

Analytical power production and cost models are developed for the series-string, MC, and MI systems. Model variables are summarized in Table I. The following subsections outline power and cost considerations for each part of the PV system and further explain each variable.

TABLE I
Model Variables

Symbol	Meaning
η_{mppt}	MPPT efficiency
η_{dcdc}	dc-dc converter efficiency
η_{inv}	inverter efficiency
χ	set of dc-dc converter sensors
ψ	set of inverter sensors
s	sensor power consumption
μ	microcontroller power consumption
C_{pv}	PV panel cost
C_{dcdc}	dc-dc converter cost
C_{inv}	inverter cost
C_s	sensor cost
C_μ	microcontroller cost

A. Power and Cost Considerations

1) PV panel: PV panel cost per watt varies with power rating. Generally, smaller rated panels cost more per watt than larger power panels. Power ratings and price were collected for a variety of PV panels. Cost per watt versus power for each panel is shown in Fig. 2. As of January 2012, the lowest retail price was $1.14 per watt for a polycrystalline Si panel, $1.28

978-1-4577-1683-6/12/$26.00 ©2012 IEEE

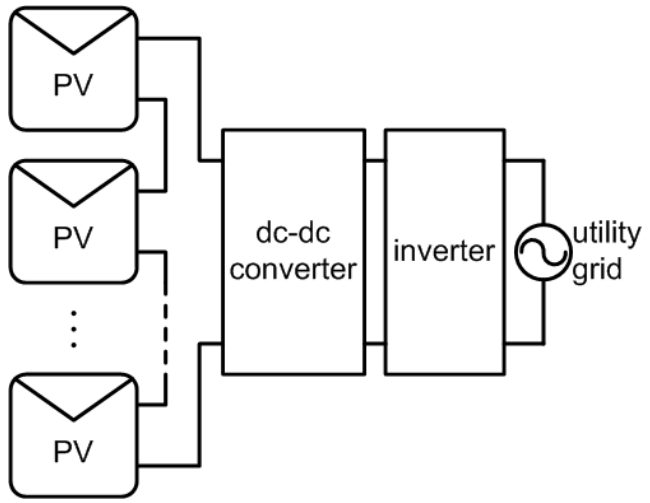

(a) PV series-string

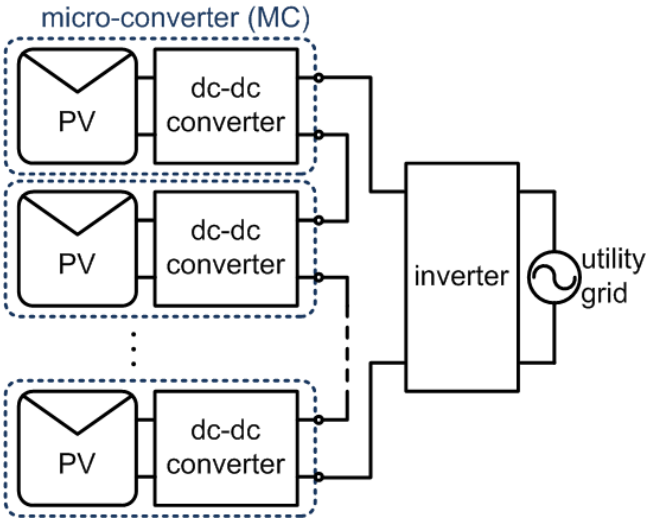

(b) PV micro-converter

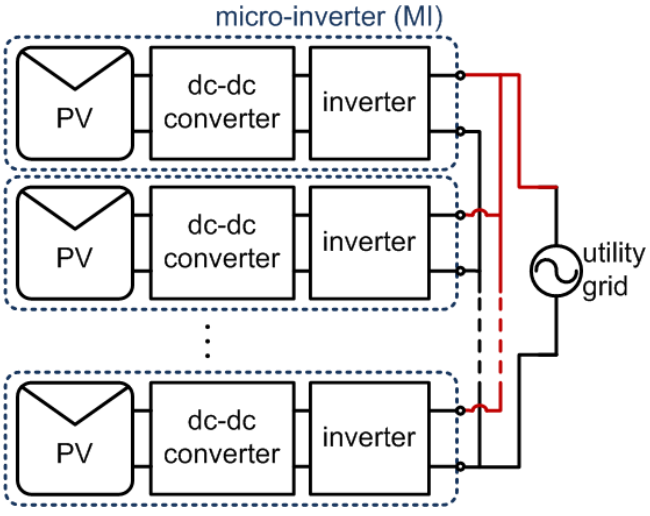

(c) PV micro-inverter

Fig. 1. Configurations for PV systems for ac applications.

per watt for a monocrystalline Si panel, and \$1.15 per watt for a thin film module [5]. Using \$1.14 per watt as a lower limit, PV cost per watt is modeled as $C_{perW} = 1.14 + 1.7 \cdot exp(-0.007 P_{pv})$, where P_{pv} is the PV panel rating. This is an optimistic price curve and assumes PV prices at lower power ratings will decrease under higher production levels. The cost of each PV panel is $C_{pv} = C_{perW} \cdot P_{pv}$.

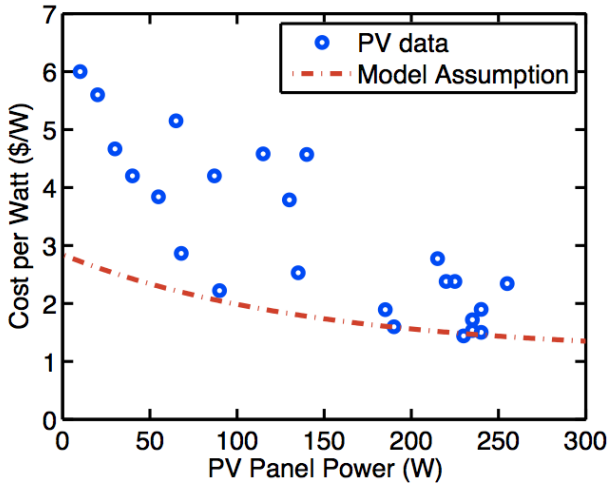

Fig. 2. Cost per watt data and model assumption for PV power ratings.

2) MPPT Efficiency: The maximum power point tracking (MPPT) efficiency variable, η_{mppt}, is the percentage of potential PV power that the panel delivers to the dc-dc converter. This value is the product of *MPP efficacy* and *tracking effectiveness*. MPP efficacy is the PV string MPP divided by the sum of each panel's MPP; it is affected by cell mismatch and shading. Tracking effectiveness depends on the MPPT method, which is used to find and maintain MPP operation.

Hill-climb perturb and observe (P&O) is a simple and commonly-used MPPT method. P&O finds the MPP by measuring PV power and updating the control set-point according to the last power measurement such that PV power is increased. *Ripple correlation control* (RCC) is an extremum-seeking method that controls operation based on PV current and voltage time derivatives. The *fractional open-circuit voltage* (FOCV) method periodically measures PV open-circuit voltage and adjusts the set-point to a fraction of that value [6]. These three MPPT algorithms have varying tracking effectiveness and will be used for different design cases. Each method also has specific sensor and controller requirements.

3) Dc-Dc Converter: The dc-dc converter implements MPPT and steps PV voltage up or down to the inverter input voltage, which is between 190 V and 400 V depending on grid ac line voltage [7]. PV series-strings reach high voltages and use buck or buck-boost converters. MICs typically use the boost topology to step up the PV module voltage [8]. Each converter has an associated efficiency that depends on loading and specific topology. A well designed converter can reach high efficiency for nominal operating conditions. This

study assumes $\eta_{dcdc} = 95\%$ for overall efficiency. Dc-dc converter base cost is assumed to be \$0.35 per watt such that $C_{dcdc} = 0.35 \cdot P_{dcdc}$, where P_{dcdc} is the power rating.

4) Inverter: Inverters are necessary in grid-tied applications to converter dc power to ac and synchronize power delivery with the grid. This study assumes $\eta_{inv} = 95\%$ is the overall inverter efficiency. As of January 2012, the lowest inverter cost was \$0.712 per watt [9]; thus, inverter base cost is $C_{inv} = 0.712 \cdot P_{inv}$, where P_{inv} is the inverter power rating.

5) Voltage and Current Sensors: Voltage and current sensors are required for converter control. The number of sensors and required accuracy depend on the specific control algorithm. The set of dc-dc converter sensors is referred to as χ. P&O and RCC require PV voltage and current measurements, while FOCV requires only PV voltage. The inverter has a set of sensors, referred to as ψ, which depend on the number of synchronized phases and type of control. Each phase requires at least one voltage sensor and one current sensor [10]. This study assumes single-phase output with one voltage and current sensor for each inverter.

Voltage is typically measured using a resistive voltage divider. Resistor cost is very low and assumed to be \$0.005. Power consumption is also minimal and assumed to be 10 μW.

There are numerous current sensing methods described in [11] and [12]. The series resistor and Hall Effect sensor are commonly used current sensors that are examined in this study. All sensing techniques consume some power and usually require signal conditioning circuitry that also consumes power. Most techniques use an amplifier to scale the sensor voltage for the analog-to-digital converter (ADC) input. This study assumes an amplifier draws 1 mA at 3 V, which is 3 mW of power, and costs \$0.05. Sensor power, s, is the sum of sensor and signal conditioning power consumption. Each sensor cost, C_s, includes the price of both the sensor and support circuitry.

Series resistor current sensing is simple and low-cost. The voltage across a small resistor that is in series with the current path is amplified and read by the microcontroller ADC. Current is calculated based on the pre-set resistance and amplification values. The power consumption, P_s, of the series resistor, R_s, is proportional to current, I_s, squared according to $P_s = I_s^2 R_s$. As current increases, power consumption increases significantly. Also, the sense resistor is connected directly to the sensed circuitry and lacks of electrical isolation. This is a disadvantage for high voltage current paths, e.g. high side current sensing in boost converters [11]. Sense resistor cost is assumed to be \$0.01 per resistor.

A Hall Effect sensor is a transducer that produces a voltage in response to a magnetic field. Current flows through a thin conductive material that is penetrated by a magnetic flux density; generated voltage is proportional to current across the sheet. Hall effect sensors provide electrical isolation between the current path and logic circuitry. It has low power consumption that is independent of current flow; this study assumes 4 mA of current at 3 V, which is 12 mW. A disadvantage of Hall Effect sensors is thermal drift, which is more prominent in MIC applications where circuitry is exposed to a range of environmental temperatures [11]. This technique requires signal conditioning circuitry to compensate for offset and scale the output. Cost is assumed to be \$1.08 per sensor.

6) Microcontroller: The microcontroller reads in sensor measurements and controls converter operation. Low microcontroller power consumption and cost become more advantageous as module number increases since overhead power can be kept low. The Texas Instruments MPS430 is a candidate for this application due to its low price and power consumption.

The MSP430 is a family of low-power microcontrollers that operate at supply voltages from 1.8 V to 3.6 V. The MSP430 microcontroller has active modes (AMs) and low-power modes (LPMs). Table II shows the modes, supply voltage and current, and power consumption for the MSP430G2x31 subfamily used in this study. The advantage of the MSP430 is that it can conserve power by "sleeping" in LPM when it is not actively making calculations and then "wake up" to take measurements and perform calculations before returning to sleep.

TABLE II
MSP430G2X31MODES AND POWER CONSUMPTION [13]

Mode	Supply Voltage (V)	Supply Current (μA)	Power (μW)
AM, 1MHz	2.2	250	550
	3.0	350	1050
AM, 100 kHz	2.2	60	132
	3.0	72	216
AM, 4 kHz	2.2	2	4.4
	3.0	3	9.0
LPM0, 1 MHz	2.2	55	121
	3.0	70	210
LPM0, 100 kHz	2.2	33	72.6
	3.0	37	111
LPM2	2.2	20	44
	3.0	22	66
LPM3	2.2	0.3	0.66
	3.0	0.7	2.1
LPM4	2.2	0.1	0.22
	3.0	0.1	0.3

In the dc-dc converter, the MPPT method determines the processing requirements, i.e., power modes and wake up frequency. Algorithms that take infrequent measurement, such as FOCV, have lower processor power consumption than those that require frequent measurements, such as RCC. Microprocessor power consumption, μ, is the percentage of time in each mode multiplied by the associated power consumption. Microcontroller cost, C_μ, is assumed to be \$0.55 for each MSP430.

B. Analytical Model

Analytical models are outlined for the MC and MI system configurations. It is assumed that there are n MICs rated for P_{in} power at the PV's MPP. The series-string configuration is the same as the MC or MI with $n = 1$.

1) Micro-Converter PV System: For n MCs, system power production, P_{sysMC}, and equipment cost, C_{sysMC}, are

$$P_{sysMC} = \left(\sum_{i=1}^{n} P_{in,i} \cdot \eta_{mppt,i} \cdot \eta_{dcdc}\right) \eta_{inv} - n\left(\sum_{j\in\chi} s_j + \mu_\chi\right) - \sum_{k\in\psi} s_k - \mu_\psi \quad (1)$$

$$C_{sysMC} = nC_{pv} + n(C_{dcdc} + \sum_{j\in\chi} C_{s,j} + C_{\mu,\chi}) + C_{inv} + \sum_{k\in\psi} C_{s,k} + C_{\mu,\psi}. \quad (2)$$

As n increases, there is a trade-off between the increased η_{mppt} due to more localized control and increased overhead power consumption and cost.

2) Micro-Inverter PV System: For n MIs, system power production, P_{sysMI}, and equipment cost, C_{sysMI}, are

$$P_{sysMI} = \sum_{i=1}^{n} P_{in,i} \cdot \eta_{mppt,i} \cdot \eta_{dcdc} \cdot \eta_{inv} - n\left(\sum_{j\in\chi} s_j + \mu_\chi + \sum_{k\in\psi} s_k + \mu_\psi\right) \quad (3)$$

$$C_{sysMI} = nC_{pv} + n(C_{dcdc} + \sum_{j\in\chi} C_{s,j} + C_{\mu,\chi}) + n(C_{inv} + \sum_{k\in\psi} C_{s,k} + C_{\mu,\psi}). \quad (4)$$

3) Cost per Watt: These equations are used to evaluate the system cost per watt, which is calculated according to

$$CpW = \frac{C_{sys}}{P_{sys}}. \quad (5)$$

The goal is to find the minimum cost per watt and associated number of modules for a variety of designs.

III. Case Studies

Analytical power and cost models are used to evaluate and compare PV system configurations for specific designs, with defined converter efficiency, MPPT method, microcontroller, current sensors, and cost. MPP efficacy is highly situational, making η_{mppt} difficult to succinctly determine. In this study, MPP efficacy is found through detailed PV panel simulations.

A. MPP Efficacy Simulation

PV panels have inherent mismatch due to variance in manufacturing and aging. Over time, total output power decreases and the variance between panel characteristics increases [14]. Forty eight 85 W PV panels with a 3% standard deviation in MPP voltage and current characteristics were modeled in Matlab using Simulink PV blocks; this represents inherent panel variation. Situational mismatch occurs under partial shading, which is represented with three irradiance cases. Case 1 is uniform 1000 W/m^2 that represents no shading. In Case 2, the top panel only is shaded at 700 W/m^2. Case 3, additionally, shades the bottom panel at 500 W/m^2 to represent a deeper shading level.

Each irradiance case is simulated on the 48 PV panels. For $n = 1$ modules, all the panels are strung in series; the string MPP is found and divided by the sum of panel MPPs to calculate MPP efficacy. Then, the string is divided into $n = 2$ and the two string MPPs are summed. This is done for $n = 1, 2, 3, 4, 6, 8, 12, 16, 24$ strings. Fig. 3 shows MPP efficacy for increasing numbers of modules under each irradiance case. In series-string configuration ($n = 1$), inherent mismatch reduces MPP efficacy to 99%, single panel shading is 97.8%, and shading two panels is 96.7%. As the number of MICs increases, MPP efficacy increases towards 100%.

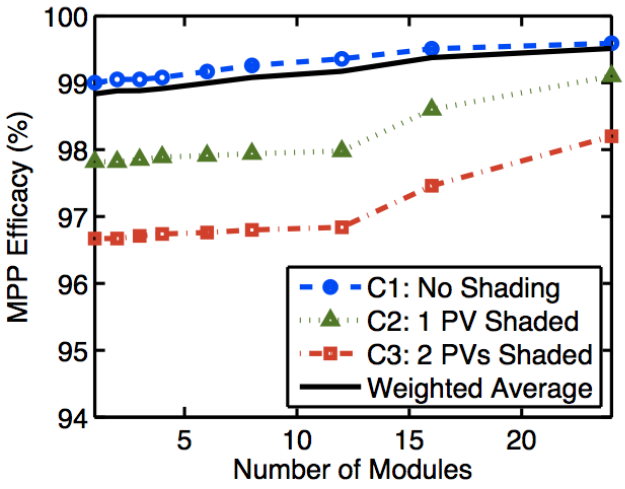

Fig. 3. MPP efficacy versus number of PV modules for a twelve-PV converter simulation under three irradiance cases.

Identifying a general MPP efficacy value is challenging because partial shading conditions vary based on location, climate, and weather conditions. For this study, assume that uniform bright conditions (Case 1) prevail for 88% of the day, single panel shading (Case 2) for 10%, and two shaded panels (Case 3) for 2%. The weighted average of these conditions is also shown in Fig. 3 and is approximated using $MPP_{efficacy} = 100 - 1.238 \cdot exp(-0.03814n)$; this value is multiplied by tracking effectiveness to determine η_{mppt}.

B. Base Case

First, consider a PV design implementing P&O. In a simulation-based study done in [15], P&O with a small step size shows around 99% MPPT tracking effectiveness; this value is used for the base case. Voltage is sensed using a voltage divider and current is sensed using a series resistor with an amplifier for signal processing. The controller is the MSP430 that operates at 3 V supply with a 100 kHz processor; 10% of the period in AM and 90% in LPM0 for an average 121.5 μW power consumption. The inverter also uses a voltage divider and series resistor plus amplifier to measure current. A separate MSP430 controls the inverter and runs at 100 kHz in AM throughout operation, drawing 216 μW.

The analytical model is used to calculate power production efficiency, system cost, and cost per watt for this base case; shown in Fig. 4 as a function of n MICs for a 10 kW rated PV system. As shown in Fig. 4(a), system efficiency is negatively affected by mismatch losses that reduces the MPPT efficiency for small n; as n increases, mismatch loss is minimized and total efficiency increases. Maximum power generation is at $n = 190$ for the MC and $n = 170$ for the MI configuration. As n further increases, incrementally increasing power consumption for sensors and the controller decreases system efficiency. Fig. 4(b) shows cost, which slowly increases until $n = 15$ modules, when the price of each PV panel greatly increases system cost. Fig. 4(c) shows system cost per watt, which reaches a minimum at $n = 9$ for both MC and MI configurations. The results indicate that from a power production perspective, a system should be divided into greater than 100 MICs to maximize power. System costs that increase significantly with n, particularly due to PV panel cost, point to much lower module numbers of around 10 to minimize cost per watt. For this range of n, there is very little performance difference between MC and MI configurations.

C. Variations from Base Case

Variations from the base case are modeled to investigate the effect of changing one design aspect. Each case is modeled using the same parameters as the base case except for the values explicitly given for the following five test cases.

1) Case A – Hall Effect Current Sensors: Case A uses Hall Effect sensors in place of series resistors for both dc-dc converter and inverter current sensing. Each sensor draws constant 4 mA at 3 V, which is 12 μW of power. The price per sensor is \$1.08, which is significantly more than the series resistor. Each Hall Effect sensor requires an amplifier that draws the same power as in the base case.

2) Case B – RCC MPPT: Case B implements RCC rather than P&O for MPPT. RCC shows slightly higher performance and is assumed to have 99.5% tracking effectiveness. Because RCC takes measurements and updates the duty ratio every switching cycle, the MSP430 in the dc-dc converter operates at 1 MHz in AM continuously, drawing 1050 μW.

3) Case C – FOCV control: Case C uses FOCV for MPPT, requiring only one voltage sensor on the PV. Tracking effectiveness is lower [15] and is assumed to be 95%. The controller in the dc-dc converter operates at 100 kHz in AM for 2% and LPM0 for 98% of the time, resulting in 40.6 μW.

4) Case D – Higher-Power Processor: Case D assumes that a controller more advanced than the MSP430 is used in the dc-dc converter that allows for additional functionality, such as communication or data logging. Assuming the controller draws 300 mA at 3 V, its power consumption is 900 mW. Cost is also higher at \$3 per controller.

5) Case E – Lower PV Cost per Watt: Case E assumes PV cost per watt is lower than the base case according to $C_{perW} = 1.14 + 0.85 \cdot exp(-0.007 P_{pv})$. The magnitude of the exponential component is half that of the base case, so there is a less significant increase at lower power ratings.

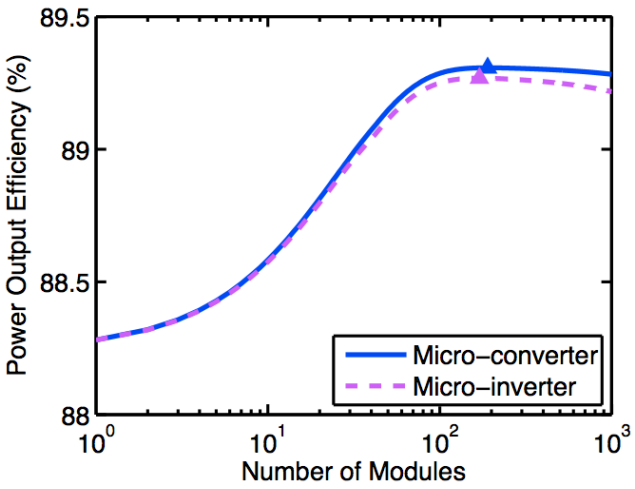

(a) power production efficiency

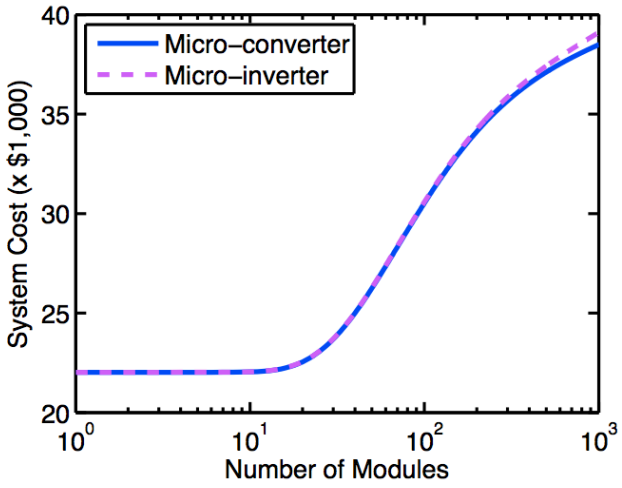

(b) system cost

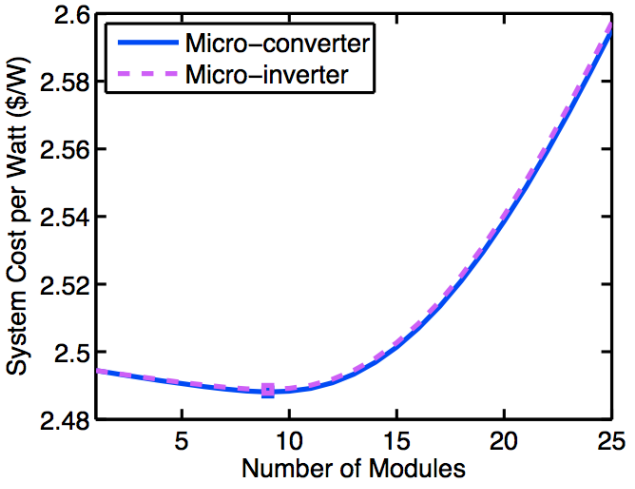

(c) system cost per watt

Fig. 4. System power production efficiency (a), cost (b), and cost per watt (c) for a 10 kW system with n MICs.

6) Results: System efficiency, cost, and cost per watt for variation Cases A through E are calculated for MC and MI configurations. MC results are shown in Fig. 5; MI results are not shown, but follow the same trends relative to the base case.

As shown in Fig. 5(a), Case A is similar to the base case, but has a slightly higher efficiency because Hall Effect sensors draw very low power. Case B shows a higher output efficiency using RCC, while Case C shows lower efficiency with FOCV. The method's tracking effectiveness directly affects overall system efficiency. Case D shows a significant efficiency drop with increasing n due to higher power consumption for the advanced controller. Case E is identical to the the base case.

System equipment cost for each case is shown in Fig. 5(b). Case B and C are identical to the base case because all components are the same. Case A and D have slightly higher cost due to the more expensive Hall Effect sensor and controller, respectively. Case E has the lowest system cost, which indicates that PV cost significantly affects system cost, particularly at higher n.

Fig. 5(c) shows system cost per watt for each case. Case A has slightly higher cost per watt than the base case implying that the lower power does not offset the higher cost. From the opposite perspective, if external design constraints require isolated current sensing, using a low-cost Hall Effect sensor does not significantly increase system cost per watt. Case D has a slightly higher cost per watt from the microprocessor cost. If higher functionality is required, cost per watt is not significantly increased for around 10 MICs. Case B has the lowest cost per watt due to high tracking effectiveness. Case C has the highest cost per watt due to low tracking effectiveness. Case E shows only a slight decrease in cost per watt; PV price would need to decrease more significantly to have a larger impact on the minimum cost per watt for the overall system.

Minimum cost per watt and the associated number of modules for each case is summarized in Table III. Note that cost per watt is based on expected performance, not the rated power; all systems are rated for 10 kW. From these results, the optimal MIC number for all design cases is in the range of 7 to 10 modules. There is a clear benefit to dividing the PV system into modules to reduce mismatch losses. Beyond 10 to 15 modules, high costs dominate and significantly increase cost per watt.

TABLE III
MINIMUM COST PER WATT AND MODULE NUMBER FOR DESIGN CASES

Case	MC		MI	
	n	**cost/W**	***n***	**cost/W**
Base	9	$2.488	9	$2.489
A: Hall Effect Sensor	9	$2.489	8	$2.491
B: RCC MPPT	9	**$2.476**	9	**$2.476**
C: FOCV MPPT	9	$2.593	9	$2.593
D: Advanced Controller	8	$2.493	7	$2.493
E: Lower PV Cost	10	$2.487	10	$2.488

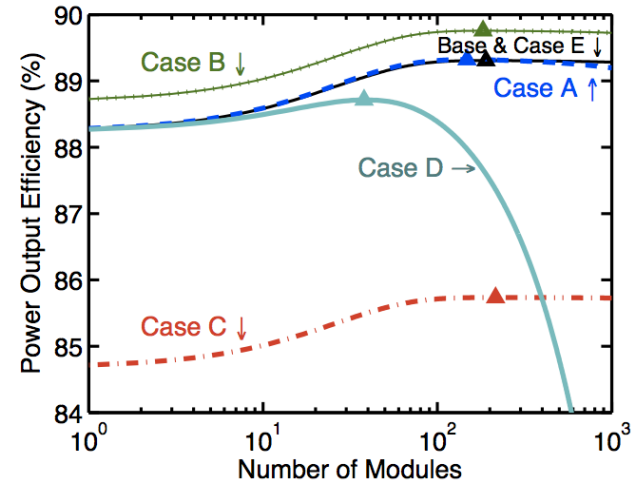

(a) power production efficiency

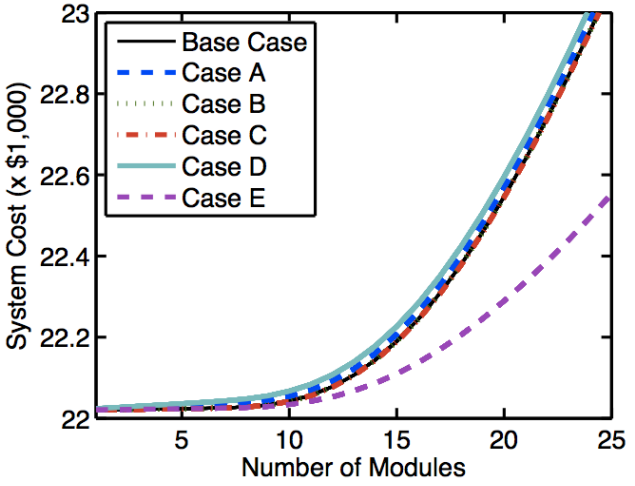

(b) system cost

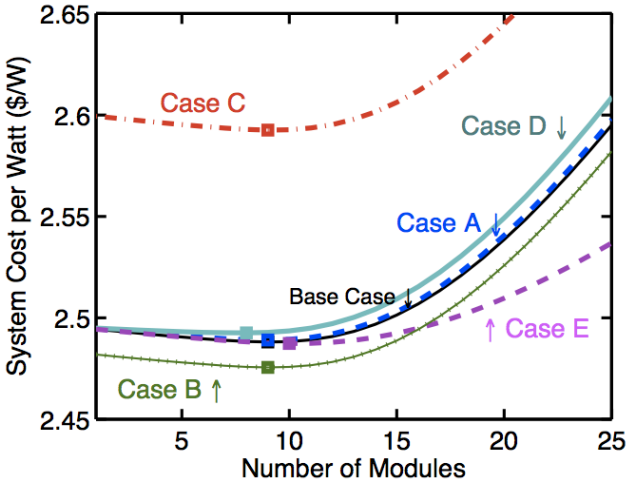

(c) system cost per watt

Fig. 5. System power production efficiency (a), cost (b), and cost per watt (c) for MC design cases.

IV. Conclusion

An analytical model is developed to compare power production and cost for series-string, MC, and MI PV systems. Design considerations include the PV panel, converter topology, number and type of sensors, microcontroller, and MPPT method. This study has examined how design aspects for PV systems affect the minimum cost per watt and corresponding number of modules. PV panel mismatch and partial shading effects significantly reduce series-string power generation, which is shown through simulation. A base case that implements P&O using a low-power microcontroller and series resistors to measure current is evaluated for a 10 kW system; optimal cost per watt is \$2.488 with 9 MCs and \$2.489 with 9 MIs. For this low range of n MICs, there is very little cost per watt difference between MC and MI configurations.

Design variations such as using Hall Effect sensors or advanced controllers result in a small cost per watt increase due to more expensive components. MPP tracking effectiveness significantly affects cost per watt; even an incremental increase in power production clearly reduces cost per watt. Among the MPPT methods, RCC showed lowest cost per watt at \$2.476 with 9 modules for both MC and MI configurations.

From this analysis, it is clear that employing a MIC approach rather than a series-string configuration reduces mismatch loss. Although output efficiency results indicate that optimal power is reached when n is greater than 100 MICs, high system costs that increase significantly with n limit the optimal cost per watt to low module numbers. PV panel cost is the main contributor, but component cost also contributes to a lesser extent. For a larger number of MICs to be cost effective, PV prices at lower power ratings must be comparable to those with higher power ratings; also, highly effective MPPT methods must be implemented with low-cost, low-power microcontrollers.

Acknowledgment

This research is supported by the Grainger Center for Electric Machinery and Electromechanics at the University of Illinois at Urbana-Champaign, the National Science Foundation through the Graduate Research Fellowship program, and Rockwell Collins through the Promoting Undergraduate Research in Engineering program.

References

[1] J. Poortmans, *et al.*, "Linking nanotechnology to gigawatts: Creating building blocks for smart PV modules," *Progress in Photovoltaics: Research and Appl.*, vol. 19, no. 7, pp. 772–780, 2011.

[2] G. Walker and J. Pierce, "Photovoltaic dc-dc module integrated converter for novel cascaded and bypass grid connection topologies - design and optimisation," in *Proc. IEEE Power Electron. Specialists Conf.*, June 2006, pp. 1–7.

[3] L. Junior, *et al.*, "Evaluation of integrated inverter topologies for low power PV systems," in *Int. Conf. on Clean Elect. Power*, June 2011, pp. 35–39.

[4] T. Esram, *et al.*, "Power electronics needs for achieving grid-parity solar energy costs," in *IEEE Energy 2030 Conf.*, Nov. 2008, pp. 1–5.

[5] Solarbuzz. (2012, Jan.) Module prices: Retail price summary - january 2012 update. [Online]. Available: http://www.solarbuzz.com/node/3184

[6] T. Esram and P. L. Chapman, "Comparison of photovoltaic array maximum power point tracking techniques," *IEEE Trans. Energy Convers.*, vol. 22, no. 2, pp. 439–449, June 2007.

[7] S. Kjaer, J. Pedersen, and F. Blaabjerg, "A review of single-phase grid-connected inverters for photovoltaic modules," *IEEE Trans. Ind. Appl.*, vol. 41, no. 5, pp. 1292 – 1306, Sept. 2005.

[8] G. R. Walker and P. C. Sernia, "Cascaded dc-dc converter connection of photovoltaic modules," *IEEE Trans. Power Electron.*, vol. 19, no. 4, pp. 1130–1139, July 2004.

[9] Solarbuzz. (2012, Jan.) Inverter prices: Retail price summary - january 2012 update. [Online]. Available: http://www.solarbuzz.com/node/241

[10] H. S. Bae, *et al.*, "New control strategy for 2-stage utility-connected photovoltaic power conditioning system with a low cost digital processor," in *Proc. IEEE Power Electron. Specialists Conf.*, June 2005, pp. 2925–2929.

[11] S. Ziegler, *et al.*, "Current sensing techniques: A review," *IEEE Sensors J.*, vol. 9, no. 4, pp. 354–376, Apr. 2009.

[12] H. P. Forghani-Zadeh and G. A. Rincon-Mora, "Current-sensing techniques for dc-dc converters," in *Midwest Symp. on Circuits and Systems*, vol. 2, Aug. 2002, pp. 577–580.

[13] "MSP430G2x31 mixed signal microcontroller datasheet," Datasheet, Texas Instruments, Dec. 2011.

[14] M. Vazquez and I. Rey-Stolle, "Photovoltaic module reliability model based on field degradation studies," *Progress in Photovoltaics: Research and Applications*, vol. 16, no. 5, pp. 419–433, 2008.

[15] R. Faranda, S. Leva, and V. Maugeri, "MPPT techniques for PV systems: Energetic and cost comparison," in *Proc. IEEE Power and Energy Society General Meeting*, July 2008, pp. 1–6.